CHEMISTRY
A EUROPEAN JOURNAL

DOI: 10.1002/chem.200401288

Self-Assembling Structures of Long-Chain Sugar-Based Amphiphiles Influenced by the Introduction of Double Bonds

Jong Hwa Jung,*[a, b] Youngkyu Do,[c] Young-A Lee,[d] and Toshimi Shimizu*[a, e]

Abstract: Nine phenyl glucoside or galactoside amphiphiles possessing a saturated or unsaturated long alkyl-chain group as the self-assembling unit of a highly organized molecular architecture were synthesized. Their self-assembly properties were investigated by using energy-filtering TEM (EF-TEM), SEM, CD, XRD, and FT-IR techniques. Compound **2**, possessing one *cis* double bond in the lipophilic portion, exhibited twisted helical fibers, which formed a bilayered structure with a 3.59 nm period, while **3** exhibited helical ribbons and left-handed nanotubular structures with 150–200 nm inner diameters and a wall thickness of approximately 20 nm. Very interestingly, **4**, possessing three *cis* double bonds, exhibited a nanotubular structure with an inner diameter of approximately 70 nm and a *d* spacing value of 4.62 nm. On the other hand, **7**, possessing two *trans* double bonds in the lipophilic region, exhibited crystal- or plate-like structures, which formed a bilayer structure with a *d* spacing value of 3.93 nm. These results indicate that the self-assembly properties are strongly dependent on the type of double bond. Furthermore, **8** and **9**, with the galactopyranose moiety, revealed helical ribbon and well-defined double helical fiber structures, respectively. These findings support the view that the orientation of the intermolecular hydrogen-bonding interaction between the sugar moieties plays a critical role in producing the nanotubular structures. According to CD and powder XRD experiments, the relatively strong intermolecular hydrogen-bonding interaction of the glucopyranoside moiety in **3** and **4** provided a highly ordered chiral packing structure. Even though these compounds formed a weak hydrophobic interaction between lipophilic groups, it led to the formation of the nanotubular structure.

Keywords: amphiphiles · carbohydrates · lipids · nanotubes · self-assembly

[a] Dr. J. H. Jung, Prof. Dr. T. Shimizu
CREST, Japan Science and Technology Corporation (JST)
Nanoarchitectonics Research Center (NARC)
National Institute of Advanced Industrial Science and Technology (AIST)
Tsukuba Central 4, 1-1-1 Higashi, Tsukuba, Ibaraki 305-8562 (Japan)
E-mail: jonghwa@kbsi.re.kr
tshmz-shimizu@aist.go.jp

[b] Dr. J. H. Jung
Nano Material Team
Korea Basic Science Institute (KBSI)
52 Yeoeun-dong, Yusung-gu, Daejeon 305-333 (Korea)
Fax: (+82) 42-865-3619

[c] Prof. Dr. Y. Do
Department of Chemistry
Korea Advanced Institute of Science and Technology (KAIST)
373-1 Guseong-dong, Yuseong-gu, Daejeon 305-701 (Korea)

[d] Prof. Dr. Y.-A Lee
Department of Chemistry
Chonbuk National University
Jeonju 561-756 (Korea)

[e] Prof. Dr. T. Shimizu
Nanoarchitectonics Research Center (NARC)
National Institute of Advanced Industrial Science and Technology (AIST)
Tsukuba Central 5, 1-1-1 Higashi, Tsukuba, Ibaraki 305-8565 (Japan)
Fax: (+81) 298-61-2659

Introduction

Currently, there is tremendous interest in high-axial-ratio nanostructures (HARNs) formed by the hierarchical self-assembly of amphiphilic molecules into helical ribbons and nanotubes.[1–6] The need for improved miniaturization and device performance in the microchip and microelectronics industry has inspired many investigations into supramolecular chemistry. It is conceivable that the "bottom-up"[7,8] HARN fabrication approach based on supramolecular chemistry will provide a solution to the anticipated size limitations of the "top-down" approach, such as photolithography,[9] thereby providing the means to fabricate ultrasmall electronic components.

In particular, the formation of organic tubular species from the aggregation of molecular species is an important nanoscience research field, since it may find applications in catalysis, selective separations sensors, and conducting devices in nano-, opto- or ionic electronics. Examples of tubular structures can be found with several organic systems, for example, lipidic,[10] peptidic,[11] and steroidic[1d,12] systems. With synthetic diacetylene lipidic systems[4] and steroids in bile,[1c,h] the average diameters of the tubular structures are

in the micrometer range, while with peptidic systems,[11] the internal cylindrical cavities are in the molecular range.

Although the evidence is limited, research has revealed[3,4,9] that tube-forming amphiphiles which mediate helical ribbons require unsaturation in the lipophilic moiety to impart a bent structure, thereby inducing supramolecular chirality. However, to the best of our knowledge, there have never been systematic studies conducted on the influence of unsaturation, that is, the number and the position of double-bond units, on the self-assembly of synthetic amphiphiles into HARNs based on solid chiral bilayers, even though the tubular structure of amphiphiles has been reported by several groups.[1,4,5,10]

We provide evidence on the self-assembled morphologies of a series of long-chain phenyl glucopyranoses, **1**–**7**, and galactopyranoses, **8**–**9**, which vary in the number of *cis* and *trans* double bonds (0–5) in their lipophilic part. The self-assembled morphologies were strongly dependent on the number of double bonds in the lipophilic regions, the types of double bonds, and the sugar moiety. The effects on the molecular packing and orientation are discussed in relation to the hydroxy group of the sugar moiety and the number of double bonds in the lipophilic region. In addition, both circular dichroism (CD) and powder X-ray diffraction (XRD) analysis provided useful information about the intermolecular chiral order. Therefore, on the basis of the CD and powder XRD experiments, we provide evidence for the chiral packing structures of self-assembling superstructures of sugar-based amphiphiles.

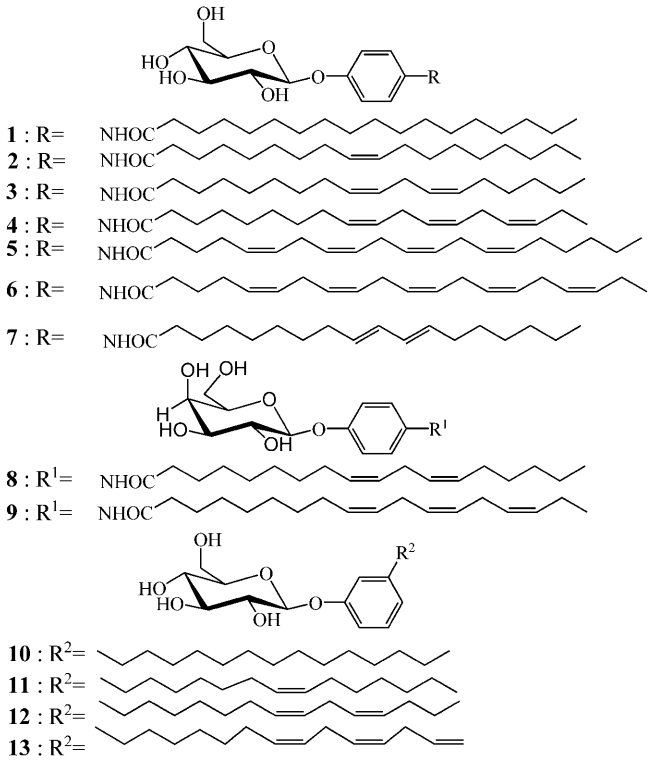

Results and Discussion

Self-assembly and morphological observations: A series of simple sugar-based amphiphiles **1**–**9** was synthesized by using a similar method to that reported previously.[13b] For self-assembly, each sugar-based amphiphile (1 mg) was dispersed in water (10–30 mL) at temperatures above the corresponding melting point, T_m, of the hydrated sample. In general, heating of the mixture at 95 °C for 30 min was enough to get a homogeneous transparent solution. The obtained aqueous solutions were allowed to cool to an incubation temperature. However, **1** was insoluble in water and only formed a typical nanofiber structure with a diameter of 100–350 nm and a length of several micrometers in a mixture of water and methanol (1:1). To characterize the resultant morphologies and their size dimensions precisely, we observed individual self-assembled structures by using energy-filtering transmission electron microscopy (EF-TEM) and scanning electron microscopy (SEM). Figure 1 displays SEM and EF-TEM images of the self-assembled structures of **2**–**9** in aqueous solution. Compound **2** exhibits a twisted fiber structure with a width of 50–200 nm and a length of several micrometers (Figure 1a). Compound **3**, however, exhibits less than 5% of a left-handed coiled tube, with a 150–200 nm inner diameter and a wall thickness of approximately 20 nm (Figure 1b), and displays a helical

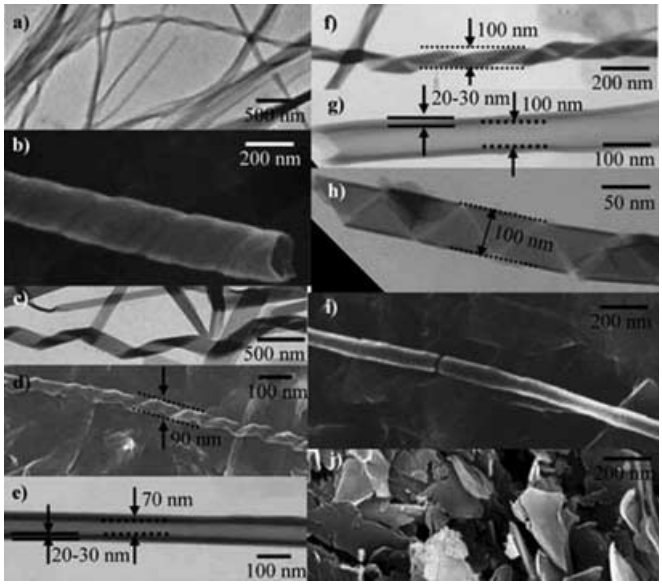

Figure 1. SEM and TEM images of self-assembled compounds a) **2**, b and c) **3**, d and e) **4**, f and g) **5**, h and i) **6**, and j) **7**.

ribbon structure (Figure 1c) as the major morphology; these results show the influence of the number of double bonds on the final morphology of the self-assembled structures.

On the other hand, **4**, possessing three *cis* double bonds in the lipophilic region, displays a helical ribbon morphology with an outer diameter of 80–100 nm as the intermediate morphology and a nanotubular structure with an inner di-

ameter of approximately 70 nm and a wall thickness of 20–30 nm as the final morphology (Figure 1 d and e). As far as can be determined, all the chiral structures possess a left-handed helical motif. These observations further support the view that the unsaturated units are important for producing nanotubes through self-assembly. Furthermore, **5** and **6** produced self-assembled solids when they reached room temperature from boiling temperature. They exhibited helical ribbons with 50–100 nm width (Figure 1 f and h) and tubular structures with an inner diameter of 80–100 nm and a wall thickness of 20–30 nm (Figure 1 g and i). These results also provide evidence that the numbers of *cis* double bonds in the lipophilic region play an important role in producing tubular structures.

To confirm the *cis*-double-bond effect in the formation of the nanotubular structure, two *trans* double bonds were introduced in the lipophilic region of **7**, in place of the *cis* double bonds of **3**. Self-assembled **7** exhibits crystal- and plate-like structures with a thickness of 160–170 nm (Figure 1 j). This result further supports the view that the morphology formation of sugar-based amphiphiles depends strongly on the types of double bonds in the long alkyl-chain group.

We also confirmed the effect of the intermolecular hydrogen-bonding interaction by the introduction of a different type of sugar moiety. Compounds **8** and **9** were synthesized with a galactose moiety instead of the glucose moiety of **3** and **4**. Compound **8** exhibited the helical ribbon structure with a width of 40–45 nm and a loose, long helical pitch (Figure 2 a and b). However, **9** forms a double-helical fiber

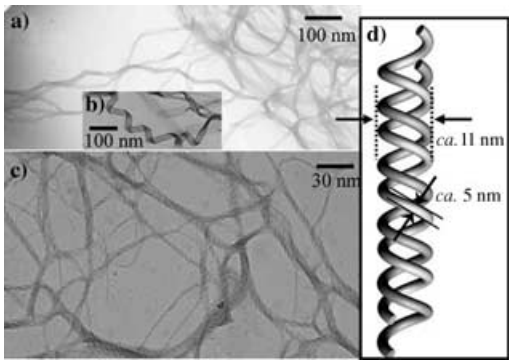

Figure 2. TEM images of self-assembled compounds a and b) **8** and c) **9**. d) Schematic representation of the left-handed double-helical fiber structure of self-assembled **9**.

structure several micrometers in length and with a diameter of approximately 11 nm (Figure 2 c and d), which exhibits a three-fold increase in the bilayer structure. All the helicity also possesses a left-handed helical motif. These findings suggest that the orientation of the intermolecular hydrogen bond is important in forming the nanostructure in water. In addition, only a few reports exist explaining the well-resolved double-helical strands or ribbons formed from chiral amphiphiles[12] and they describe only metastable intermediate molecular assemblies, which slowly convert into highly ordered structures. To the best of our knowledge, the present finding also gives a unique example of a stable nanometer-sized double-helical structure.

Chiral self-assembly involved a helically coiled ribbon structure as an intermediate. After hot aqueous dispersions of nanotube-forming amphiphiles are cooled, there are two routes for nanotube formation. One route proceeds with shortening of the helical pitch of the ribbon and maintaining a constant ribbon width, whereas the second involves widening of the helical width and maintaining a constant helical pitch. Figure 3 shows the SEM images: self-assembled **4** pos-

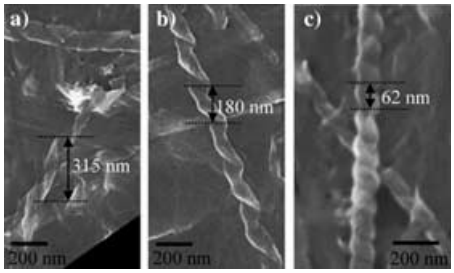

Figure 3. SEM images of the self-assembled helical ribbons obtained from **4**.

sesses the helical ribbon structure with various pitchs (62–315 nm) and with a constant ribbon width (approximately 80 nm) in the initial stage. Also, as far as can be determined, all the helicity possesses a left-handed helical motif. The latter observation is more common in the literature than the former. These findings strongly suggest that the sugar-based organic tube formed by self-assembly was produced by a change of pitch length of the helical ribbon with a constant ribbon width, as depicted in Figure 4 a, rather than by the mechanism represented in Figure 4 b. This mechanism is quite different from that observed for the crown-appended cholesterol tube,[14] which formed by the mechanism depicted in Figure 4 b. Perhaps the formation mechanisms for tubular structures are related to the formation conditions, cooling times, and deriving forces. However, it is not currently clear what the main factor is in deciding the mechanism of tube formation.

CD measurement: As alternative evidence for the nanotube formation of **3** and **4** in the microscopic structural view, we carefully observed the CD spectra of the self-assembled compounds **2**–**4** and **7**–**9** (Figure 5). The CD spectra of the self-assembled compounds **3** and **4** in aqueous solution showed a strong negative band at 237 (Figure 5 bb) and 225 nm (Figure 5 c), respectively, on forming the nanotubular structures with chiral assembly. They showed only a weak CD signal at temperatures above a phase-transition temperature (Figure 5 d and e) and this was shifted to a longer wavelength; this signal probably corresponds to a monomers or small lipid aggregates, such as micelles or vesi-

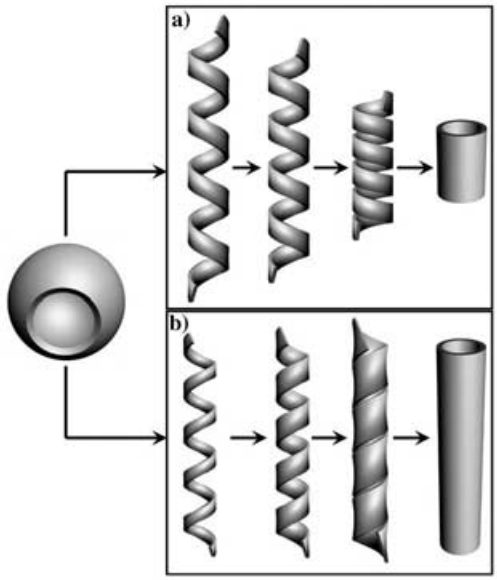

Figure 4. Representation of possible tube-formation mechanisms of **4**: a) the tube is formed by a change in the pitch length; b) the tube is formed by growth in the width of the helical ribbon.

Table 1. Self-assemblies with different morphologies and their physical data.

Compound	T_{gel} [°C][a]	Morphology[b]	*d* spacing [nm][c]	Molecular length [nm][d]
1	–	fiber structure	–	–
2	90.0	twisted fiber structure	3.59	3.03
3	65.2	helical ribbon structure	4.62	3.15
4	–	tubular structure	4.62	3.02
5	50.1	tubular structure	–	–
6	–	tubular structure	–	–
7	–	plate-like structure	3.93	3.20
8	–	helical ribbon structure	3.87	3.03
9	–	double-helical fiber structure	3.81	3.15
10	–	twisted fiber structure	–	–
11	47.8	tubular structure	–	–
12	17.4	–	–	–
13	−25.4	–	–	–

[a] From differential scanning calorimetry (DSC) data. [b] From EF-SEM observations. [c] From XRD data. [d] From molecular modeling.

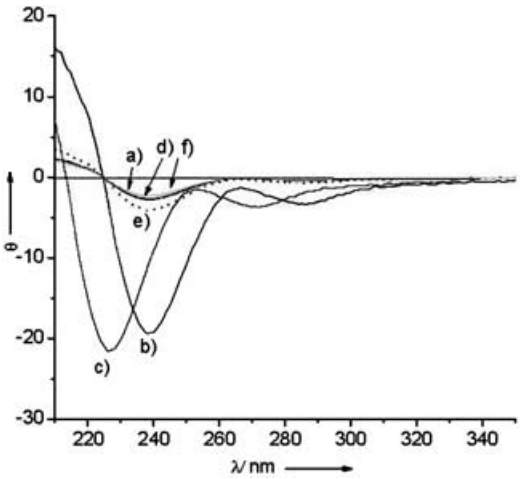

Figure 5. CD spectra of self-assembled compounds a) **2**, b) **3**, c) **4**, all at 25.0 °C, d) **3** at 70.0 °C, e) **4** at 70.0 °C, and f) **7** at 25.0 °C.

cles. The CD signal, however, became strong again when the lipid self-assembled to form nanotubular structures after several hours. However, the CD spectrum of self-assembled **2** in aqueous solution showed a much weaker negative band (Figure 5a) in comparison to that of **3** and **4**, thereby suggesting that self-assembled **2** forms disordered chiral packing structures. These CD spectroscopy results provide direct evidence for the chiral molecular architecture of nanotubes and for the fact that the molecular packing of **3** and **4** is loosely chiral at temperatures above the phase-transition temperature. Furthermore, the phase-transition temperatures of **3** and **4** are much higher (Table 1) than those of glucoside amphiphiles **11**–**13**, which lack the amide group,[10b] a fact indicating that stabilization of self-assembled tubes of **3** and **4** is enhanced mainly by intermolecular hydrogen-bonding interactions between the amide groups.

Since the gel-to-liquid crystalline phase-transition temperature was near room temperature for self-assembled **5** and **6**, we could not obtain enough information on the chiral packing structures or the number of *cis* double bonds influencing the formation of the helical ribbon and the tubes by CD spectrscopy.

The CD spectrum of self-assembled **7**, possessing two *trans* double bonds, was measured as a reference to confirm the effect of *cis* double bonds in the formation of the tubular structure (Figure 5f). The CD intensity of self-assembled **7** was much smaller than that of **4**. This result indicates that the sugar moiety of **7** formed loose chiral packing with intermolecular hydrogen-bonding interactions between the glucose moieties, which is due to the relatively strong hydrophobic interaction between the linear long alkyl-chain groups.

The CD spectra of the galactose-based amphiphiles **8** and **9**, with two and three *cis* double bonds, respectively, were also measured to obtain information regarding chiral molecular packing structures with changed sugar moieties. The galactose-based amphiphiles **8** and **9** formed helical ribbon and double-helical fiber structures, which appeared in the CD spectra as negative bands at 238 nm (Figure 6a and b). The CD intensities were smaller than those of **3** and **4**. These results continue to support the view that galactose-based amphiphiles **8** and **9** form disorderly chiral packing structures with a hydrophobic interaction that is stronger than those formed by glucose-based amphiphiles **3** and **4**.

Powder XRD measurement: Recently, an X-ray crystallographic method for ascertaining the molecular packing of self-assemblies has been reported,[1d,f,10] and this method was

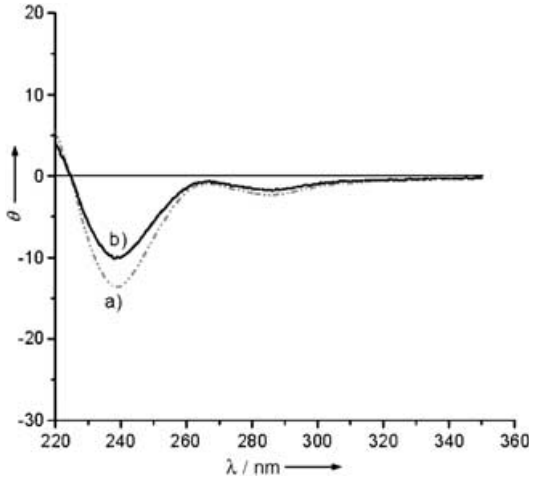

Figure 6. CD spectra of self-assembled compounds a) **9** and b) **8** at 25.0 °C.

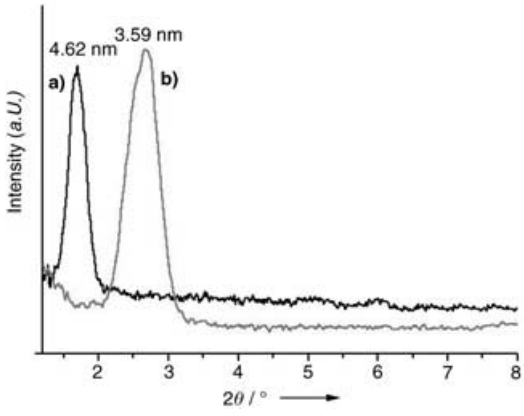

Figure 7. Powder XRD pattern values in the small-angle region of the freeze-dried nanostructures from a) **4** and b) **2**.

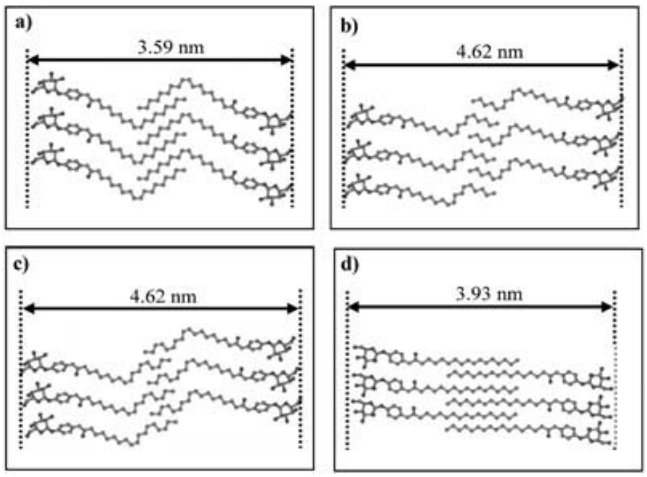

Figure 8. Possible molecular arrangements of the self-assembled compounds a) **2**, b) **3**, c) **4**, and d) **7**.

used to clarify the self-assembly mechanism. First, the molecular length of three amphiphiles was calculated by using Corey–Pauling–Koltun (CPK) modeling based on single-crystal data for oleic, linoleic, and linolenic acid.[15] The models showed similar values despite a bending effect. Second, X-ray diffraction patterns were measured. The *d* spacing values of crystalline **2**–**9** from the self-assembly are shown in Table 1 and Figure 7. The small-angle diffraction patterns of helical ribbons of **3** and nanotubes of **4** appeared at 4.62 nm (Figure 7a and Table 1), which is smaller than twice the extended molecular length of **3** (3.15 nm by using the CPK molecular modeling) and **4** (3.02 nm) but larger than the length of one molecule. These results strongly suggest that self-assembled **3** and **4** form a bilayer structure with a relatively small region interdigitated by hydrophobic interaction, as shown in Figure 8b and c. On the other hand, the diffraction diagram of the microcrystalline solid **2** (length of one molecular according to the CPK molecular modeling: 3.03 nm) indicated a bilayer structure with a *d* value of 3.59 nm (Figure 8a), a result supporting the theory that **2** maintains a much stronger interdigitated bilayer structure between the lipophilic regions than those of **3** and **4**.

Furthermore, the *d* value (3.93 nm) for self-assembled **7**, possessing *trans* double bonds in the long alkyl chain, is much smaller than that of self-assembled **3** (Table 1). This finding indicates that the molecular packing of the plate-like structure obtained from **7** forms a relatively stronger hydrophobic interaction with the interdigitated bilayer structure (Figure 8d) between the lipophilic regions than that of **3** or **4**.

The *d* values of galactose-based amphiphiles **8** and **9** were also smaller than those of glucose-based amphiphiles **3** and **4**, a result indicating again that amphiphiles **8** and **9** form a relative strong hydrophobic interaction with a large region of interdigitated bilayer structure in the lipophilic section. Once again, according to CD spectroscopy and powder X-ray diffraction results, the relatively strong intermolecular hydrogen-bonding interactions of the glucopyranoside moiety of **3** and **4** provide a highly ordered chiral packing structure, even though these compounds form a weak hydrophobic interaction between the lipophilic groups, which led to the formation of the nanotubular structure.

IR measurement: Compound **2** shows a highly ordered structure in the aliphatic region, possibly due to hydrocarbon crystallization, an observation which is further supported by the Fourier transformation infrared (FT-IR) spectroscopy studies showing C–H stretching values of 2855 cm^{-1} for **3**/**4** and 2851 cm^{-1} for **2** (Table 2). It is reasonable to

Table 2. FT-IR results of the self-assembled compounds **1**–**4**.

compound	CH_2 [cm^{-1}]	C=O [cm^{-1}]
1	2851	1657
2	2851	1656
3	2855	1649
4	2855	1649

argue that the lipophilic groups of **3** and **4**, possessing three *cis* double bonds, formed a more disordered structure than that of **2**. Also, the C=O (amide I) stretching patterns of the three compounds **2**–**4** are different: the signals for **3** and **4** appeared at 1649 cm^{-1}, whereas that for **2** appeared at 1656 cm^{-1}. This suggests that **3** and **4** maintain a well-ordered structure of the glucopyranoside head group by intermolecular hydrogen-bonding interactions between the amide groups.

Conclusion

The present study has demonstrated that long-chain phenyl glucosides form twisted nanofiber, helical ribbon, and nanotubular structures, depending on the double-bond unsaturation. Long-chain phenyl galactosides revealed that their helical ribbon and double-helical fiber structures depended on the number of double bonds. *cis* double bonds in the lipophilic region of long-chain phenyl glucosides more efficiently induce the tubular structure, compared to *trans* double bonds. To the best of our knowledge, these results are the first example of a systematic study of the influence of *cis* double-bond units in a hydrophobic portion on self-assembled morphologies. Based on the CD results, the self-assembled nanotubular structure showed a relatively stronger intensity than that of the twisted fiber structure, a fact indicating that the nanotubes formed relatively well-ordered chiral packing structures compared to the twisted fiber structures. Furthermore, the XRD experiments indicated that the relatively weak hydrophobic interactions of the glucopyranoside moiety of **3** and **4** formed bilayer structures between the lipophilic groups, which led to the formation of the nanotubular structure.

Experimental Section

General: The ^1H and ^{13}C NMR spectra were recorded with a JEOL 600 (600 MHz) or a JEOL GSX 270 (270 MHz) NMR spectrometer. Preparative column chromatography was performed on silica gel. The chromatographic purity of the intermediates was monitored by thin-layer chromatography (Kiesel gel F 254, Merck). The compounds were visualized by spraying the plates with 5% sulfuric acid in methanol and then charring them on a hot plate. The molecular lengths were estimated by molecular mechanics calculations performed with the CONFLEX-MM2 force field as implemented in the CAChe program, version 4.1.1 (Fujitsu Co. Ltd., Japan).

TEM observations: The aqueous dispersions of the nanostructures (0.1 mg mL^{-1}) were dripped onto an amorphous carbon grid and excess water was blotted with filter paper. TEM was performed with a Carl-Zeiss LEO912 instrument operated at 50 keV. Images were recorded on an imaging plate (Fuji Photo Film Co. Ltd. FDL5000 system) with 20 eV energy windows at 3000–250000× and were digitally enlarged.

FT-IR measurements: The FT-IR spectra of the self-assembled nanostructures were measured with a JASCO FT-620 FT-IR spectrometer operated at 4 cm^{-1} resolution with an unpolarized beam and attenuated total reflection (ATR) accessory system (Diamond Miracle horizontal ATR accessory with a diamond crystal prism, PIKE Technologies, USA) and a mercury cadmium telluride (MCT) detector. Several drops of the aqueous dispersions of the nanotube (0.1 mg mL^{-1}) were dripped onto the prism and dried under a nitrogen stream prior to measurement.

XRD measurements: The XRD pattern of a freeze-dried sample was measured with a Rigaku type 4037 diffractometer by using graded *d*-space elliptical side-by-side multilayer optics, monochromated CuKα radiation (40 kV, 30 mA), and an R-Axis IV imaging plate. The typical exposure time was 10 min with a 150 mm camera length. Freeze-dried samples of **2**–**9** were vacuum dried to constant weight and then put into capillary tubes, without being powdered.

1-Octadecanecarboxylic chloride: A mixture of 1-octadecanecarboxylic acid (0.15 g, 0.58 mmol), oxalic chloride (0.50 g, 3.96 mmol), and dimethylformamide (DMF; 1–2 drops) was dissolved in dichloromethane (5.0 mL), and the reaction mixture was then stirred for 10 h at room temperature. The residual oxalic chloride and solvent were removed by vacuum. The product was directly used for the coupling reaction without further purification.

Related carboxylic chlorides were synthesized according to a similar method.

***p*-Aminophenyl-β-D-glucopyranoside** and ***p*-Aminophenyl-β-D-galactopyranoside**: *p*-Nitrophenyl-β-D-glucopyranoside (1.0 g, 2.54 mmol) or *p*-nitrophenyl-β-D-galactopyranoside (1.0 g, 2.54 mmol) was dissolved in methanol (150 mL). 10% Pd/C (1.0 g) was then added to the solution. Hydrogen gas was introduced into the mixed solution for 10 h at room temperature under a nitrogen atmosphere. The reaction mixture was filtered to remove Pd/C, and the filtrate was evaporated in vacuo to dryness. The residue was purified by column chromatography on silica gel with tetrahydrofuran (THF)/chloroform (1/1): Yields 80–90%; ^1H NMR (600 MHz, [D_6]DMSO): $\delta = 3.4$–4.1 (s, 2H), 5.2–5.3 (m, 3H), 5.6 (s, 1H), 6.7 (d, 2H), 7.37–7.46 ppm (m, 5H); FT-IR (KBr): $\tilde{\nu} = 3312$, 2909, 1635, 1510, 1364, 1217, 1089, 1005, 1035, 999, 806, 706 cm^{-1}; MS (*p*-nitrobenzoic acid (NBA)): *m*/*z*: 360 $[M+H]^+$; elemental analysis calcd (%) for $C_{19}H_{21}NO_6$: C 63.50, H 5.89, N 3.90; found: C 63.18, H 6.04, N 3.78.

Octadecanoyl-*p*-aminophenyl-β-D-glucopyranoside (1): A mixture of *p*-aminophenyl-β-D-glucopyranoside (0.30 g, 1.10 mmol), dodecanoyl choride (0.24 g, 1.10 mmol), and triethylamine (0.536 g, 5.50 mmol) in dry THF (50 mL) was heated to reflux for 3 h under a nitrogen atmosphere. The solution was filtered after cooling to room temperature, and the filtrate was concentrated to dryness by a vacuum evaporator. The residue was purified by column chromatography on silica gel with methanol/chloroform (1:6): Yield 40%; ^1H NMR (600 MHz, [D_6]DMSO): $\delta = 0.9$ (t, 3H), 1.2–2.0 (m, 24H), 2.3 (m, 2H), 3.2–4.7 (m, 19H), 7.25 (d, 2H), 7.65 (d, 2H), 9.1 ppm (s, 1H); FT-IR (KBr): $\tilde{\nu} = 3340$, 2912, 1630, 1510, 1364, 1217, 1089, 1005, 1035, 999, 806, 706 cm^{-1}; MS (NBA): *m*/*z*: 538.27 $[M+H]^+$; elemental analysis calcd (%) for $C_{30}H_{51}NO_7$: C 67.01, H 9.56, N 2.60; found: C 67.20, H 9.25, N 2.55.

Related compounds (**2**–**9**) were synthesized according to a similar method. Their analytical data are described below.

***n*-(11′*Z*)-Octadecanyl-(*p*-aminophenyl-β-D-glucopyranoside) (2)**: Yield 50%; m.p. 127.5°C; ^1H NMR (600 MHz, [D_6]DMSO): $\delta = 0.9$ (t, 3H), 1.2–2.5 (m, 20H), 3.2–4.7 (m, 21H), 4.82 (d, 2H), 7.25 (d, 2H), 7.65 (d, 2H), 9.1 ppm (s, 1H); FT-IR (KBr): $\tilde{\nu} = 3410$, 3340, 2915, 1630, 1513, 1357, 1217, 1090, 1005, 1035, 999, 806, 706 cm^{-1}; MS (NBA): *m*/*z*: 536.55 $[M+H]^+$; elemental analysis calcd (%) for $C_{30}H_{49}NO_7$: C 67.26, H 9.22, N 2.61; found: C 67.52, H 9.40, N 2.52.

***n*-(9′*Z*,12′*Z*)-Octadecadienyl-(*p*-aminophenyl-β-D-glucopyranoside) (3)**: Yield 50%; m.p. 120.7°C; ^1H NMR (600 MHz, [D_6]DMSO): $\delta = 0.9$ (t, 3H), 1.2–3.0 (m, 18H), 3.2–4.7 (m, 21H), 4.82 (d, 2H), 7.25 (d, 2H), 7.65 (d, 2H), 9.1 ppm (s, 1H); FT-IR (KBr): $\tilde{\nu} = 3410$, 3342, 2912, 1628, 1513, 1364, 1219, 1089, 1005, 1035, 999, 806, 706 cm^{-1}; MS (NBA): *m*/*z*: 534.73 $[M+H]^+$; elemental analysis calcd (%) for $C_{30}H_{47}NO_7$: C 67.51, H 8.88, N 2.62; found: C 67.31, H 8.50, N 2.57.

***n*-(6′*Z*,9′*Z*,12′*Z*)-Octadecatrienyl-(*p*-aminophenyl-β-D-glucopyranoside) (4)**: Yield 63%; m.p. 105.5°C; ^1H NMR (600 MHz, [D_6]DMSO): $\delta = 0.9$ (t, 3H), 1.2–2.5 (m, 20H), 3.2–4.7 (m, 21H), 4.82 (d, 2H), 7.25 (d, 2H), 7.65 (d, 2H), 9.1 ppm (s, 1H); FT-IR (KBr): $\tilde{\nu} = 3410$, 3342, 2912, 1630, 1511, 1367, 1217, 1089, 1007, 1035, 999, 806, 706 cm^{-1}; MS (NBA): *m*/*z*:

532.80 $[M+H]^+$; elemental analysis calcd (%) for $C_{30}H_{45}NO_7$: C 67.77, H 8.53, N 2.63; found: C 67.25, H 8.55, N 2.50.

***n*-(5′*Z*,8′*Z*,11′*Z*,14′*Z*-Dosocatetraenyl-(*p*-aminophenyl-β-D-glucopyranoside) (5)**: Yield 55%; m.p. 65.7°C; ^{1}H NMR (600 MHz, [D$_6$]DMSO): $\delta =$ 0.9 (t, 3H), 1.2–2.5 (m, 20H), 3.2–4.7 (m, 21H), 4.82 (d, 2H), 7.25 (d, 2H), 7.65 (d, 2H), 9.1 ppm (s, 1H); FT-IR (KBr): $\tilde{\nu}=3412$, 3341, 2912, 1633, 1512, 1365, 1215, 1089, 1003, 1035, 999, 806, 706 cm^{-1}; MS (NBA): *m*/*z*: 558.75 $[M+H]^+$; elemental analysis calcd (%) for $C_{32}H_{47}NO_7$: C 68.91, H 8.49, N 2.51; found: C 69.05, H 8.53, N 2.47.

***n*-(5′*Z*,8′*Z*,11′*Z*,14′*Z*,17′*Z*)-Dosocapentaenyl-(*p*-aminophenyl-β-D-glucopyranoside) (6)**: Yield 57%; m.p. 52.5°C; ^{1}H NMR (600 MHz, [D$_6$]DMSO): $\delta=0.9$ (t, 3H), 1.2–2.5 (m, 20H), 3.2–4.7 (m, 21H), 4.82 (d, 2H), 7.25 (d, 2H), 7.65 (d, 2H), 9.1 ppm (s, 1H); FT-IR (KBr): $\tilde{\nu}=3412$, 3345, 2913, 1630, 1510, 1364, 1217, 1089, 1007, 1035, 999, 806, 707 cm^{-1}; MS (NBA): *m*/*z*: 556.55 $[M+H]^+$; elemental analysis calcd (%) for $C_{32}H_{45}NO_7$: C 69.16, H 8.16, N 2.52; found: C 69.15, H 8.73, N 2.42.

***n*-(*trans*,*trans*-9′,11′)-Octadecadienyl-(*p*-aminophenyl-β-D-glucopyranoside) (7)**: Yield 50%; m.p. 170.5°C; ^{1}H NMR (600 MHz, [D$_6$]DMSO): $\delta=0.9$ (t, 3H), 1.2–3.0 (m, 18H), 3.2–4.7 (m, 21H), 4.82 (d, 2H), 7.25 (d, 2H), 7.65 (d, 2H), 9.1 ppm (s, 1H); FT-IR (KBr): $\tilde{\nu}=3413$, 3341, 2913, 1630, 1512, 1365, 1217, 1089, 1005, 1035, 999, 806, 706 cm^{-1}; MS (NBA): *m*/*z*: 534.73 $[M+H]^+$; elemental analysis calcd (%) for $C_{30}H_{47}NO_7$: C 67.51, H 8.88, N 2.62; found: C 67.45, H 8.65, N 2.54.

***n*-(9′*Z*,12′*Z*)-Octadecadienyl-(*p*-aminophenyl-β-D-galactopyranoside) (8)**: Yield 60%; m.p. 150.5°C; ^{1}H NMR (600 MHz, [D$_6$]DMSO): $\delta=0.9$ (t, 3H), 1.2–3.0 (m, 18H), 3.2–4.7 (m, 21H), 4.82 (d, 2H), 7.25 (d, 2H), 7.65 (d, 2H), 9.1 ppm (s, 1H); FT-IR (KBr): $\tilde{\nu}=3410$, 3340, 2912, 1630, 1510, 1364, 1217, 1089, 1005, 1035, 999, 806, 706 cm^{-1}; MS (NBA): *m*/*z*: 534.73 $[M+H]^+$; elemental analysis calcd (%) for $C_{30}H_{47}NO_7$: C 67.51, H 8.88, N 2.62; found: C 67.01, H 9.01, N 2.54.

***n*-(6′*Z*,9′*Z*,12′*Z*)-Octadecatrienyl-(*p*-aminophenyl-β-D-galactopyranoside) (9)**: Yield 55%; m.p. 125.9°C; ^{1}H NMR (600 MHz, [D$_6$]DMSO): $\delta=0.9$ (t, 3H), 1.2–2.5 (m, 20H), 3.2–4.7 (m, 21H), 4.82 (d, 2H), 7.25 (d, 2H), 7.65 (d, 2H), 9.1 ppm (s, 1H); FT-IR (KBr): $\tilde{\nu}=3410$, 3345, 2917, 1630, 1517, 1364, 1215, 1088, 1007, 1035, 999, 806, 706 cm^{-1}; MS (NBA): *m*/*z*: 532.80 $[M+H]^+$; elemental analysis calcd (%) for $C_{30}H_{45}NO_7$: C 67.77, H 8.53, N 2.63; found: C 68.25, H 8.55, N 2.50.

Acknowledgements

We thank the CREST of JST (Japan Science and Technology) for financial support. In addition, J.H.J. is grateful to KOSEF for partial financial support.

[1] a) T. Kunitake, *Angew. Chem.* **1992**, *104*, 692; *Angew. Chem. Int. Ed. Engl.* **1992**, *31*, 709; b) J.-H. Fuhrhop, W. Helfrich, *Chem. Rev.* **1993**, *93*, 1562; c) J.-H. Fuhrhop, J. Koning, *Membranes and Molecular Assembles: The Synkinetic Approach* (Ed.: J. F. Stoddart), The Royal Society of Chemistry Cambridge, **1994**; d) J. H. Jung, H. Kobayashi, M. Masuda, T. Shimizu, S. Shinkai, *J. Am. Chem. Soc.* **2001**, *123*, 8795; e) T. Shimizu, *Macromol. Rapid Commun.* **2002**, *23*, 311; f) R. Oda, I. Huc, M. Schmutz, S. J. Candau, F. C. Mackintosh, *Nature* **1999**, *399*, 566; g) G. Li, W. Fudickar, M. Skupin, A. Klyszcz, C. Draeger, M. Lauer, J.-H. Fuhrhop, *Angew. Chem.* **2002**, *114*, 1906; *Angew. Chem. Int. Ed.* **2002**, *41*, 1828; h) D. S. Chung, G. B. Benedek, F. M. Konikoff, J. M. Donovan, *Proc. Natl. Acad. Sci. USA* **1993**, *90*, 11341.

[2] a) J. D. Hartgerink, E. Beniash, S. I. Stupp, *Science* **2001**, *294*, 1684; b) S. I. Stupp, V. LeBonheur, K. Walker, L. S. Li, K. E. Huggins, M. Keser, A. Amstutz, *Science* **1997**, *276*, 384.

[3] a) J. S. Cheng, S. Kopta, R. C. Stevens, *J. Am. Chem. Soc.* **2001**, *123*, 3205; b) Q. Cheng, M. Yamamoto, R. C. Stevens, *Langmuir* **2000**, *16*, 5333.

[4] a) M. S. Spector, A. Singh, P. B. Messersmith, J. M. Schnur, *Nano Lett.* **2001**, *1*, 375; b) M. S. Spector, J. V. Selinger, A. Singh, J. M. Rodriguez, R. R. Price, J. M. Schnur, *Langmuir* **1998**, *14*, 3493; c) M. S. Spector, R. R. Price, J. M. Schnur, *Adv. Mater.* **1999**, *11*, 337; d) J. M. Schnur, B. R. Ratna, J. V. Selinger, A. Singh, G. Jyothi, K. R. Easwaran, *Science* **1994**, *264*, 945; e) M. S. Spector, K. R. Easawaran, G. Jyothi, J. V. Seliger, A. Singh, J. M. Schnur, *Proc. Natl. Acad. Sci. USA* **1996**, *93*, 12943; f) J. M. Schnur, *Science* **1993**, *262*, 1669.

[5] G. John, M. Mason, P. M. Ajayan, J. S. Dordick, *J. Am. Chem. Soc.* **2004**, *126*, 15012.

[6] a) B. K. Mishra, B. N. Thomas, *J. Am. Chem. Soc.* **2002**, *124*, 6866; b) B. N. Thomas, C. R. Safinya, R. J. Plano, N. A. Clark, *Science* **1995**, *267*, 1635; c) B. N. Thomas, R. C. Cororan, C. L. Cotant, C. M. Lindeman, J. E. Kirsch, P. J. Persichini, *J. Am. Chem. Soc.* **2002**, *124*, 1227; d) S. Pakhomov, R. P. Hammer, B. K. Mishra, B. N. Thomas, *Proc. Natl. Acad. Sci. USA* **2003**, *100*, 3040.

[7] a) O. Gronwald, S. Shinkai, *Chem. Eur. J.* **2001**, *7*, 4329; b) S. Sakurai, S. Shinkai, *J. Am. Chem. Soc.* **2000**, *122*, 4520; c) K. Yoza, N. Amanokura, Y. Ono, T. Akao, H. Shinmori, M. Takeuchi, S. Shinkai, D. N. Reinhoudt, *Chem. Eur. J.* **1999**, *5*, 2722; d) N. Amanokura, Y. Kanekiyo, S. Shinkai, D. N. Reinhoudt, *J. Chem. Soc. Perkin Trans. 2* **1999**, 1995.

[8] a) M. Schmutz, B. Michels, P. Marie, M. P. Krafft, *Langmuir* **2003**, *19*, 4889; b) S. Wang, R. Lunn, M. P. Krafft, R. M. Leblanc, *Langmuir* **2000**, *16*, 2882; c) S. M. Bertilla, J.-L. Thomas, P. Marie, M. P. Krafft, *Langmuir* **2004**, *20*, 3920; d) M. Maaloum, P. Muller, M. P. Krafft, *Langmuir* **2004**, *20*, 2261.

[9] Y. Xia, G. M. Whitesides, *Angew. Chem.* **1998**, *110*, 568; *Angew. Chem. Int. Ed.* **1998**, *37*, 550.

[10] a) G. John, M. Masuda, Y. Okada, K. Yase, T. Shimizu, *Adv. Mater.* **2001**, *13*, 715; b) G. John, J. H. Jung, H. Minamikawa, K. Yoshida, T. Shimizu, *Chem. Eur. J.* **2002**, *8*, 5494; c) B. Yang, S. Kamiya, H. Yui, M. Masuda, T. Shimizu, *Chem. Lett.* **2003**, *32*, 1146; d) J. H. Jung, G. John, K. Yoshida, T. Shimizu, *J. Am. Chem. Soc.* **2002**, *124*, 10674.

[11] a) D. T. Bong, T. D. Clark, J. R. Granja, M. R. Ghadiri, *Angew. Chem.* **2001**, *113*, 1016; *Angew. Chem. Int. Ed.* **2001**, *40*, 988; b) S. Ferandez-Lopez, H.-S. Kim, E. C. Choi, M. Delgado, J. R. Granja, A. Khasanov, K. Krehenbuehl, G. Long, D. A. Weinberger, K. M. Wilcoxen, M. R. Ghadiri, *Nature* **2001**, *412*, 452.

[12] a) P. Terech, Y. Talmon, *Langmuir* **2002**, *18*, 7240; b) P. Terech, A. de Geyer, B. Sernd, Y. Talmon, *Adv. Mater.* **2002**, *14*, 495.

[13] a) R. Iwaura, K. Yoshida, M. Masuda, M. Ohnish-Kameyama, M. Yoshida, T. Shimizu, *Angew. Chem.* **2003**, *115*, 1039; *Angew. Chem. Int. Ed.* **2003**, *42*, 1009; b) J. H. Jung, K. Yoshida, T. Shimizu, *Langmuir* **2003**, *19*, 8724.

[14] J. H. Jung, S.-H. Lee, J. S. Yoo, K. Yoshida, T. Shimizu, S. Shinkai, *Chem. Eur. J.* **2003**, *9*, 5307.

[15] J. Ernst, W. S. Sheldrick, J.-H. Fuhrhop, *Z. Natuforsch.* **1979**, *34b*, 706.

Received: December 16, 2004
Published online: July 11, 2005

